Pergamon

Geochimica et Cosmochimica Acta, Vol. 68, No. 8, pp. 1723–1733, 2004

0016-7037/04 $30.00 + .00

doi:10.1016/j.gca.2003.10.018

Vanadium(V) adsorption onto goethite (α-FeOOH) at pH 1.5 to 12: A surface complexation model based on ab initio molecular geometries and EXAFS spectroscopy

CAROLINE L. PEACOCK and DAVID M. SHERMAN*
Department of Earth Sciences, University of Bristol, Bristol, BS8 1RJ, UK

(*Received September* 12, 2002; *accepted in revised form October* 8, 2003)

Abstract—We measured the adsorption of V(V) onto goethite (α-FeOOH) under oxic (P_{O2} = 0.2 bar) atmospheric conditions. EXAFS spectra show that V(V) adsorbs by forming inner-sphere complexes as $VO_2(OH)_2$ and $VO_3(OH)$. We predicted the relative energies and geometries of $VO_2(O, OH)_2$-FeOOH surface complexes using ab initio calculations of the geometries and energetics of analogue $Fe_2(OH)_2(H_2O)_6O_2VO_2(O, OH)_2$ clusters. The bidentate corner-sharing complex is predicted to be substantially (57 kJ/mol) favoured energetically over the hypothetical edge-sharing bidentate complex. Fitting the EXAFS spectra using multiple scattering shows that only the bidentate corner-sharing complex is present with Fe-V and V-O distances in good agreement with those predicted. We find it important to include multiple scattering in the fits of our EXAFS data otherwise spurious V-Fe distances near 2.8 Å result which may be incorrectly attributed to edge-sharing complexes. We find no evidence for monodentate complexes; this agrees with predicted high energies of such complexes. Having identified the $Fe_2O_2V(OH)_2^+$ and $Fe_2O_2VO(OH)^0$ surface complexes, we are able to fit the experimental vanadium(V) adsorption data to the reactions

$$2FeOH_2^+ + VO_2^+ = Fe_2O_2V(OH)_2^+ + 2H^+$$

and

$$2FeOH + HVO_4^{2-} = Fe_2O_2VO(OH)^0 + 2OH^-$$

We also determined the first acid dissociation constant of the $Fe_2O_2VO_2H_2^+$ surface complex.

Fits of sorption edges to surface complexation models are ambiguous. This is one of the first studies to provide a surface complexation model of sorption edges that is consistent with both spectroscopic and quantum mechanical constraints.

1. INTRODUCTION

Vanadium exists in the +3, +4 and +5 oxidation states under aqueous conditions (Fig. 1) with the +5 oxidation state stable in oxic seawater. In dilute solutions, the dominant species of vanadium(V) are the phosphate-like mononuclear vanadate oxyanions ($VO_2(OH)_2^-$ and $VO_3(OH)^{2-}$) (Wehrli and Stumm, 1989, Wanty and Goldhaber, 1992). In more concentrated solutions, vanadium(V) can form polynuclear species (Cruywagen and Heyns, 1991). At concentrations in excess of ~100 μmol/L V, solution species can include those of decavanadate ($H_xV_{10}O_{28}^{x-6}$) and metavanadate ($(VO_3)_x^{x-}$) form (Baes and Mesmer, 1976). At concentrations in excess of ~0.1 mol/L V, decavanadates, metavanadates and pyrovanadates (e.g., $V_2O_7^{4-}$) replace the mononuclear oxyanions as the primary species of V(V) (Baes and Mesmer, 1976).

The aqueous geochemistry of vanadium is strongly controlled by both redox state and sorption onto iron oxide and clay minerals. Adsorption of V(V) onto colloidal iron oxides produced at hydrothermal vents at mid ocean ridges limits the concentration of vanadium in seawater (Trefry and Metz, 1989; Elderfield and Schultz, 1996). Sorption onto ferric oxyhydroxides in particulate matter controls the chemistry of vanadium in the English Channel (Auger et al., 1999). Sorption onto minerals also regulates vanadium concentration in groundwater systems (Breit and Goldhaber, 1989; Northrop and Goldhaber, 1990; Wanty et al., 1990; Wanty and Goldhaber, 1992; Breit, 1995; Schwertmann and Pfab, 1996). Of the iron oxides, goethite and hematite are the most thermodynamically stable (Langmuir, 1997).

There have been few molecular investigations of the interaction of aqueous vanadium with oxide minerals. Wehrli and Stumm (1988, 1989) investigated the adsorption of vanadium (IV and V) onto TiO_2 and δ-Al_2O_3 via surface complexation modelling, adopting the approach of Hohl and Stumm (1976). The adsorption of vanadium(V) reflected the complex solution chemistry of these species (Fig. 1). At low pH, inner-sphere surface complexation of the VO_2^+ cation was proposed despite electrostatic repulsion from a positively charged oxide surface. A similarly strong sorption of the monovalent neptunyl(V) dioxocation ($Np(V)O_2^+$) was reported by Keeney-Kennicutt and Morse (1984). At higher pH, inner-sphere surface complexation was proposed via the adsorption of HVO_4^{2-}. The vanadate anion behaves like phosphate and can specifically adsorb via ligand exchange (Sigg and Stumm, 1980). Wehrli and Stumm (1988, 1989) therefore reported an adsorption envelope for the adsorption of vanadium(V) to TiO_2 and δ-Al_2O_3. Kurbatov plots of the V(V) adsorption envelope revealed a slope of $n = 1$ suggesting the formation of predominantly monodentate surface complexes.

Few studies have attempted to develop a surface complex-

* Author to whom correspondence should be addressed (dave.sherman@bristol.ac.uk).

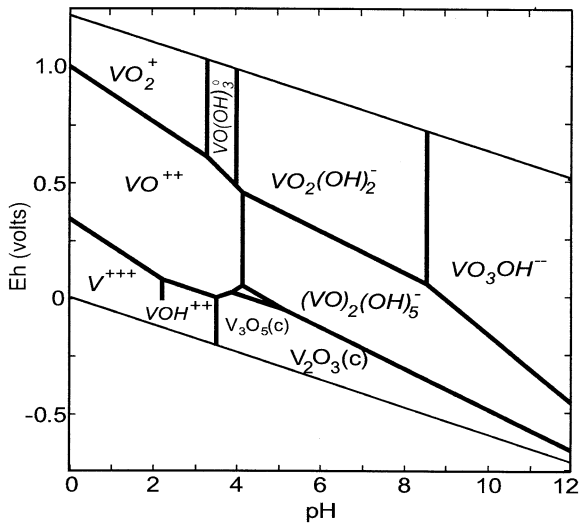

Fig. 1. Eh-pH diagram for vanadium aqueous species in the system V-O-H. $[V]_{total} = 5 \times 10^{-5}$ *m* (~2.5 ppm); hence, no polymer species are stable.

ation model constrained by results from spectroscopy. On the other hand, EXAFS spectra of surface complexes can be difficult to interpret. To this end, we use first-principles (density functional theory) calculations of surface complex geometries. Through direct spectroscopic observation, with interpretation aided by ab initio calculation, we provide a molecular-level understanding of V(V) adsorption to goethite that is used to develop a rigorous surface complexation model.

The goal of the work reported here is to determine the mechanism by which vanadium(V) sorbs to goethite (α-FeOOH) and to determine realistic surface complex stability constants that can be used for geochemical modelling.

2. EXPERIMENTAL METHODS

2.1. Mineral Preparation and Characterisation

Goethite was prepared by hydrolysis of a $Fe(NO_3)_3$ solution at pH 12 to 13 and 70°C for 60 h (Schwertmann and Cornell, 1991). Mineral identity and purity was confirmed by X-ray powder diffraction (XRD) analysis of randomly orientated powder samples. The surface area of the synthesised goethite was measured by BET to be 32.7 ± 3 m^2/g.

2.2. Potentiometric Titration

Goethite potentiometric titrations were carried out at three salt concentrations (0.003, 0.01 and 0.1 mol/L $NaNO_3$) following the method of Hayes et al. (1991). Dried solid goethite was suspended in preboiled, nitrogen-purged (<1 ppm CO_2(g)) 18.2-mΩ MilliQ water and nitrogen-purged (<1 ppm CO_2(g)) overnight before titrations. Initial pH after overnight purging was ~8. Titrations were performed at 25°C in an air-tight reactor with constant stirring to prevent settling. Base (NaOH, free from carbonate), acid (HNO_3) and salt solutions ($NaNO_3$) were prepared from stock solutions and added via an automated titrator. A nitrogen atmosphere (<1 ppm CO_2(g)) was maintained throughout the experiment. Electrolyte was added to adjust the ionic strength to 0.003 mol/L and acid then added to gradually lower the pH to ~4 (see Hayes et al., 1991). Incremental addition of base then produced a titration from pH ~4 to 11. After each incremental addition of base, 5 min were allowed for pH equilibration. The suspension was returned to pH ~ 4 by reverse acid titration, electrolyte added to adjust the ionic strength to the next level and the titration repeated following the same method. Goethite concentration in solution was 6.63 g/L. In agreement with similar titration studies (e.g., Hayes et al., 1991; Robertson and Leckie, 1998; Venema et al., 1998) we observed no significant hysteresis between the acid and base titration legs.

We used a pin-tip double junction glass combination electrode (Sentek) with a salt bridge of 3 mol/L $NaNO_3$. The electrode was calibrated potentiometrically following the method of Gans and Sullivan (2000).

The base leg of the titration is reported here and is used to optimise acid-base parameters for use in goethite-vanadium surface complexation modelling.

2.3. Sample Synthesis

2.3.1. Adsorption of V(V) onto goethite

Goethite batch experiments were prepared with vanadium(V) aqueous solution using AR grade reagents and 18.2-mΩ MilliQ water. All solutions and resulting experimental suspensions were purged with N_2(g) (<1 ppm CO_2(g)) and all adsorption experiments were conducted at 25°C.

Vanadium(V) stock solution was prepared at 100 ppm from $NaVO_3$(s). Batch experiments with 25 ppm $[V]_{total}$ were prepared by adding 7.5 mL of 100 ppm V stock solution to 0.1 g goethite in 22.5 mL of 0.1 mol/L $NaNO_3$. Goethite concentration in solution was therefore 3.33 g/L. Batch experiments with 2.5 ppm $[V]_{total}$ were prepared by adding 10 mL of 100 ppm V stock solution to 0.03 g goethite in 30 mL of 0.1 mol/L $NaNO_3$. Goethite concentration in solution was therefore 0.75 g/L. The resulting suspensions were immediately shaken and initial pH was recorded after stabilisation to two decimal places. Suspension pH was then varied from pH 1.5 to 12 by the dropwise addition (<1 mL) of HNO_3/NaOH and recorded after stabilisation to two decimal places. Batch experiments were then shaken continuously for 144 h. V(V) was adsorbed under oxic ($P_{O2} = 0.2$ bar) atmospheric conditions. Adsorption of V(V) to goethite at 25 and 2.5 ppm $[V]_{total}$ was investigated with EXAFS spectroscopy of specific samples from the adsorption edge at pH ~ 3, 6 and 8. At 25 ppm $[V]_{total}$, goethite samples at pH ~ 3, 6 and 8 contained 0.74, 0.65 and 0.49 wt.% vanadium with estimated surface coverage (calculated assuming 6.02 sites/nm^2 and 32.73 m^2/g) at 44.5, 39 and 29.7%, respectively. At 2.5 ppm $[V]_{total}$, goethite samples at pH ~ 3, 6 and 8 contained 0.33, 0.33 and 0.32 wt.% vanadium with surface coverage at 19.7, 20.1 and 19.3%, respectively.

Batch adsorption samples were separated by centrifugation (10,000 rpm for 10–15 min) into an adsorption sample (thick paste) for spectroscopic analysis and a clear supernate for determination of total vanadium concentration. Supernates were filtered using 0.2-μm cellulose nitrate membrane filters, acidified with 1% HNO_3 before filtering and analysed for vanadium by inductively-coupled plasma atomic emission spectrometry (ICP-AES). All adsorption samples were spectroscopically analysed either immediately after centrifugation or after storage at 1 to 4°C for a maximum of 48 h.

2.4. EXAFS Data Collection and Analysis

2.4.1. Data collection

EXAFS fluorescence spectra of the vanadium K edge (4.95 keV) were collected on station 8.1 at the CLRC Synchrotron Radiation Source, Daresbury Laboratory, UK. Adsorption samples were presented to the X-ray beam as a wet paste held by Sellotape in a 2-mm-thick Teflon slide with a 4 × 15 mm sample slot. A vanadium(V) stock solution sample was also analysed after 144 h to ensure vanadium oxidation state did not change during the timescale of our experiments. During data collection, storage ring energy was 2.0 GeV and the beam current varied between 130 and 240 mA. The monochromator was set to reject 50% of the incoming beam to minimise higher harmonics in the EXAFS spectrum. EXAFS data were collated from up to 10 fluorescence mode scans using an Ortec 18-element solid state detector.

It should be noted that EXAFS cannot discriminate between V and Fe using phase and amplitude functions alone. Next-nearest neighbour distances in section 3.1 are therefore Fe or V.

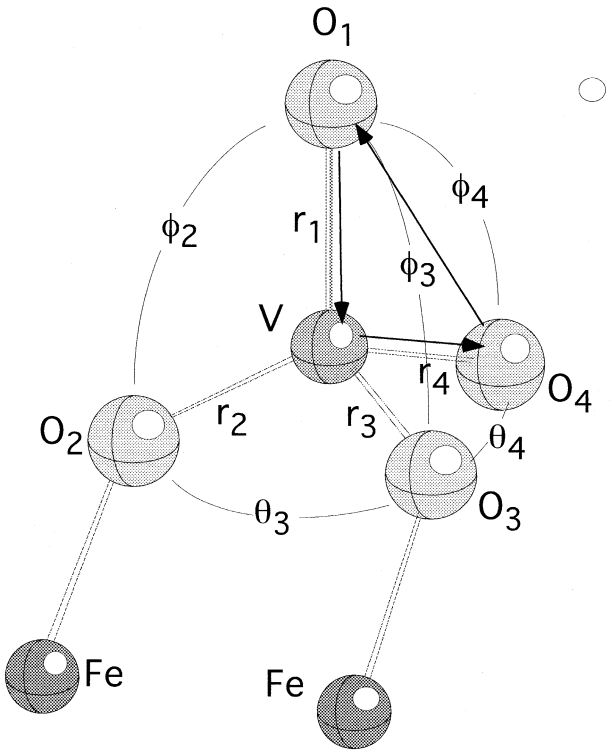

Fig. 2. Multiple scattering configuration used in EXAFS fits for V(V) sorbed to goethite.

2.4.2. Data analysis

EXAFS data reduction was performed using Daresbury Laboratory software (EXCALIB and EXBACK, Dent and Mosselmans, 1992). EXCALIB was used to calibrate from monochromator position (millidegrees) to energy (eV) and to average multiple spectra from individual samples. EXBACK was used to define the start of the EXAFS oscillations (determined from the inflection point on the K edge) and perform background subtraction. The preedge was fit to a linear function and the postedge background to two 2nd-order polynomial segments. EXAFS were fit in the small atom approximation and we allowed for multiple scattering as coded in EXCURV98 (Binsted, 1998). Multiple scattering paths were limited to those involving three atoms as longer paths had no effect. The phase-shift functions used in the curve fitting were derived by ab initio methods in EXCURV98 using Hedin-Lundqvist potentials (Hedin and Lundqvist, 1969) and von Barth ground states. The inclusion of multiple scattering improved the fit in the 2.5- to 3.5-Å region where some of the features result from O-O scattering within the VO_4^{3-} tetrahedra. Multiple scattering calculations require specification of the full three dimensional structure of the V coordination environment (i.e., bond angles in addition to bond lengths). This was done using a hypothetical model cluster (Fig. 2) with C1 symmetry. Note that the multiple-scattering contributions were calculated self-consistently during the EXAFS fits. No Fourier filtering was performed during the data analysis and all shells were fit with no constraints to the Debye-Waller factor and distances.

2.5. Density Functional Calculations

Quantum mechanical calculation of cluster geometries and energies were performed using the ADF 2.0 code of te Velde et al. (2001) which implements density functional theory for finite clusters and molecules using the linear combination of atomic orbital formalism. Molecular orbitals in the ADF code are constructed from Slater-type atomic orbitals, consisting of a Cartesian part $r^{kr}x^{kx}y^{ky}z^{kz}$ with $k_x + k_y + k_z = l$ (where l is the angular momentum quantum number) and an exponential part $e^{-\alpha r}$. Density functional theory allows a very large basis set to be used: For all atoms we used an uncontracted, triple-zeta basis set with polarisation functions (i.e., 1s2s2p3s3p3d3d′3d″4s4s′4s″ + 4p for iron, 1s2s2s′2s″ + 3d for oxygen, 1s2s2p3s3p3d3d′3d″4s4s′4s″ + 4p for vanadium and 1s1s′1s″ + 2p for hydrogen). The charge density was also fit to a Slater-type orbital basis set. For all atoms except hydrogen, we used frozen core orbitals (i.e., 1s, 2s, 2p and 3p for Fe; 1s for O; and 1s, 2s, 2p and 3p for V).

We used the Vosko et al. (1980) parameterisation for the local exchange-correlation functionals together with generalised gradient corrections of Perdew et al. (1992). All calculations were performed using the spin-unrestricted formalism and we set the cluster to have a ferromagnetic configuration. The choice of ferromagnetic vs. antiferromagnetic configuration for the $Fe_2(OH)_2(H_2O)_8$ substrate should only have a minor chemical effect. (Note that a spin-restricted calculation would be seriously in error, however, since it would mix in configurations associated with high energy multiplets as discussed by Sherman [1985].)

The geometries of the clusters were optimised using a Newton-Raphson method and Broydon-Fletcher update of the Hessian matrix as coded in ADF 2.0. During the geometry optimisations the total energies were converged to ±5 kJ/mol.

2.6. Surface Complexation Modelling

The program FITEQL v3.2 (Herbelin and Westall, 1996) was used to fit the acid-base behaviour of the goethite surface and subsequently the adsorption behaviour of vanadium on goethite to a surface complexation model. The diffuse layer model (DLM) (Dzombak and Morel, 1990) and triple layer model (TLM) (Hayes and Leckie, 1987; Hayes et al., 1988) were used to account for surface electrostatics. FITEQL is used extensively for the calculation of chemical equilibrium constants in metal adsorption studies (e.g., Lovgren et al., 1990; Hayes et al., 1991; Jung et al., 1998; Robertson and Leckie, 1998; Ikhsan et al., 1999; Tadanier and Eick, 2002). The quality of the fits produced is given by

$$V(Y) = (Y/S_Y)^2/(n_p \times n_{II} - n_u) \quad (1)$$

where Y is the actual error in the mass balance equation, S_Y is the estimated experimental error given by FITEQL and the reciprocal of the variance S_Y is the weighting factor. n_p is the number of data points, n_{II} is the number of chemical components with known total and free concentrations, and n_u is the number of adjustable parameters (Lumsdon and Evans, 1994; Gao and Mucci, 2001). A reasonably good fit to experimental metal binding data is indicated by a value of $V(Y)$ between 0.1 and 20 (Herbelin and Westall, 1996).

3. RESULTS AND DISCUSSION

3.1. Sorption of V(V) on Goethite

The conjugate acids of the vanadate anion are the dominant vanadium species in the Eh-pH range of natural oxic waters (Fig. 1). We measured the sorption of V(V) to α-FeOOH from pH 1.5 to 12 at 2.5 and 25 ppm $[V]_{total}$. At 2.5 ppm, only mononuclear V(V) solution species form; at 25 ppm, both mononuclear and polynuclear V(V) solution species form.

The speciation of V^{5+} at 2.5 ppm $[V]_{total}$ and over the pH range investigated is shown in Figure 3. At low pH, V^{5+} occurs as the VO_2^+ cation (Fig. 3) which is specifically adsorbed to the positively charged FeOOH surface despite electrostatic repulsion (in agreement with Wehrli and Stumm, 1988, 1989). At higher pH, V^{5+} exists as conjugate acids of the VO_4^{3-} anion (Fig. 3). $VO_2(OH)_2^-$ and $VO_3(OH)^{2-}$ react like phosphate and sorb to the negatively charged FeOOH surface by ligand exchange (Sigg and Stumm, 1980). Hence we find an adsorption envelope at each $[V]_{total}$ (Fig. 4). The shape of the adsorption envelope resulting from the 2.5 ppm $[V]_{total}$ solution is in excellent agreement with previous studies of V(V) sorp-

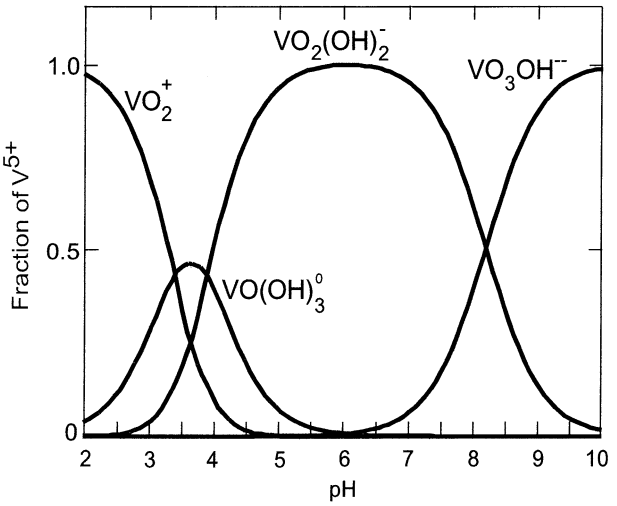

Fig. 3. Speciation of vanadium(V) as a function of pH. $[V]_{total} = 5 \times 10^{-5}$ *m* (~2.5 ppm) in 0.1 mol/L $NaNO_3$.

tion onto anatase (TiO_2) and δ-Al_2O_3 (Wehrli and Stumm, 1988, 1989).

The adsorption of V(V) onto goethite also shows a concentration dependence at higher pH: adsorption at 25 ppm $[V]_{total}$ is somewhat less between pH ~6 and 9 compared to adsorption at 2.5 ppm $[V]_{total}$ in the same pH range. The solution speciation of vanadium(V) at 25 ppm includes polynuclear V(V) species, namely decavanadates (e.g., $V_{10}O_{27}(OH)^{5-}$) between pH ~3 and 5 and metavanadates (e.g., $V_3O_9^{3-}$) between pH ~5 and 8 (Baes and Mesmer, 1976). We therefore tentatively attribute decreased adsorption between pH ~6 and 9 at 25 ppm $[V]_{total}$ to the formation of metavanadate species (e.g., $V_3O_9^{3-}$) in solution (see surface complexation modelling discussed below).

3.1.1. V K-Edge EXAFS spectroscopy

V K-edge EXAFS (and Fourier transforms of the EXAFS) for wet-paste goethite adsorption samples at 2.5 and 25 ppm $[V]_{total}$ are shown in Figures 5 and 6 respectively and summarised in Table 1. At both lower and higher total vanadium concentrations and over the pH range subject to spectroscopy, EXAFS results indicate the formation of a common surface complex consistent with either ($VO_2(OH)_2^-$) or ($VO_3(OH)^{2-}$) vanadate groups. At pH ~ 3, 6 and 8 we find ~4.0 O at ~1.5 to 1.8 Å consistent with the protonated tetrahedral VO_4^{3-} ion as $VO_2(OH)_2^-$ or $VO_3(OH)^{2-}$. From ab initio cluster geometries (discussed below) we predict that a completely unprotonated VO_4 group on the goethite surface gives V-O bond lengths too long compared to those seen in the EXAFS. Furthermore, the surface complexation model (discussed below) is consistent with the formation of doubly protonated surface vanadium groups (at low pH, 1–4) and singly protonated surface vanadium groups (at higher pH, 4–12).

We assign the next-nearest neighbour distances of 3.2 and

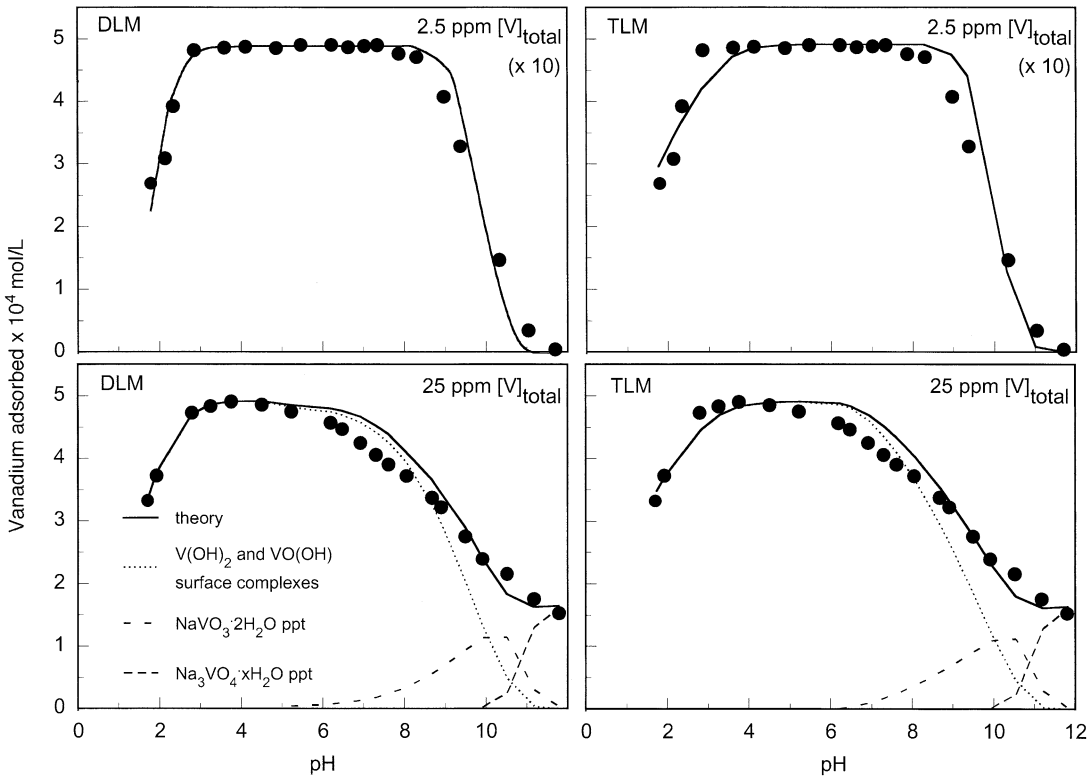

Fig. 4. Adsorption of vanadium(V) ions to goethite (α-FeOOH) at $I = 0.1$ $NaNO_3$ and 25°C, shown as total vanadium adsorbed in mol/L after 144 h equilibration time; 3.33 g/L oxide, 2.5 ppm and 25 ppm $[V]_{total}$. Symbols are data points, lines are surface complexation model fits.

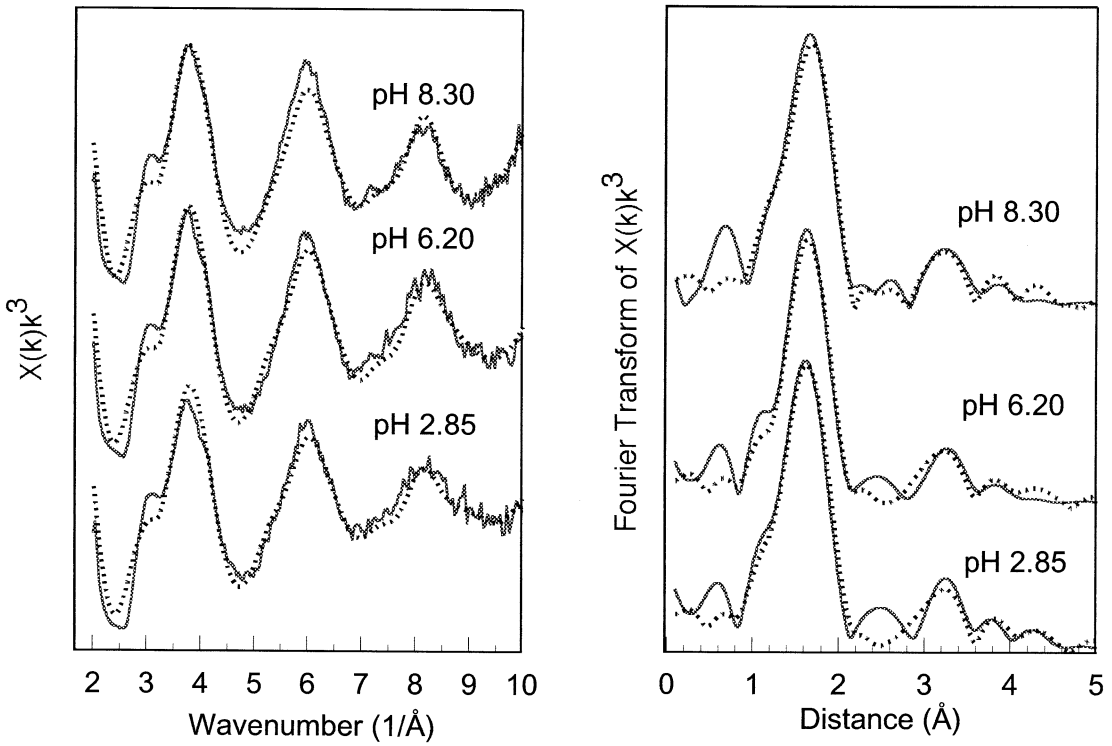

Fig. 5. EXAFS and Fourier transform of EXAFS for V(V) adsorption samples equilibrated with 2.5 ppm $[V]_{total}$.

3.3 Å to $VO_2(O, OH)_2$ bidentate corner-sharing complexes between $VO_2(O, OH)_2$ and two edge-sharing FeO_6 polyhedra (Figs. 7b and 7c, see discussion below). We only find evidence for the formation of bidentate corner-sharing complexes on the α-FeOOH surface. If multiple scattering is not included, we find a spurious V-Fe distance at 2.8 Å that would be assigned to edge-sharing between $VO_2(O, OH)_2$ and FeO_6 polyhedra.

3.1.2. Predicted geometries and energetics of V(V) surface complexes from Ab initio molecular geometries

Calculated geometries for clusters analogous to bidentate edge-sharing and bidentate corner-sharing surface complexes are shown in Figure 7. We predicted the relative energies and geometries of clusters analogous bidentate edge- and corner-sharing surface complexes of $VO_2(OH)_2$, $VO_3(OH)$ and VO_4. The bidentate corner-sharing complexes would form on the {110} and {010} faces of goethite (using setting Pbnm) while the bidentate edge-sharing complexes could form on the {021} and {001} faces. However, the bidentate edge-sharing $VO_2(OH)_2$ complex (Fig. 7a) is energetically unfavourable by 57 kJ/mol relative to the bidentate corner-sharing $VO_2(OH)_2$ complex (Fig. 7b). This energy difference is too large to allow any significant contribution from the edge-sharing surface complex. Furthermore, this prediction is in agreement with our EXAFS that show two nearest-neighbour V-Fe distances and evidence for only bidentate corner-sharing complexes. We find the $VO_2(OH)_2$ corner-sharing complex is more stable (by 76 kJ/mol) if the protons are on the V oxygens (i.e., $Fe_2O_2V(OH)_2$ rather than $Fe_2(OH)_2VO_2$). This is consistent with our surface complexation model (discussed below). Predicted molecular geometries show that a completely unprotonated VO_4 on the α-FeOOH surface (Fig. 7d) gives V-O bond lengths too long compared to those seen in the EXAFS spectra (Table 1). The bond lengths in both the $Fe_2O_2V(OH)_2^+$ and $Fe_2O_2VO_2H^0$ surface complexes however (Figs. 7b and 7c) are in reasonable agreement with those seen via EXAFS (Table 1). We therefore attribute V(V) surface adsorption to the formation of bidentate corner-sharing $Fe_2O_2V(OH)_2^+$ and $Fe_2O_2VO(OH)^0$surface complexes.

The formation of inner-sphere bidentate corner-sharing complexes on the α-FeOOH surface rather than edge-sharing complexes is in agreement with the results found for As on iron(III) oxyhydroxides (Sherman and Randall, in press).

3.2. Surface Complexation Modelling

3.2.1. Equilibria at the mineral surface

The goethite mineral surface was modelled using the single-site two-p*K* model, where the single surface adsorption site may exist in one of three protonation states: SOH_2^+, SOH and SO^-. A homogeneous mineral surface with only one type of active surface functional group was assumed. Surface acidity constants were assigned to the reactions

$$SOH + H^+ = SOH_2^+ \qquad \log K_{a1} \tag{2}$$

and

$$SOH = SO^- + H^+ \qquad \log K_{a2} \tag{3}$$

where S is a non-specific surface metal ion and SOH_2^+, SOH and SO^- are representative surface species.

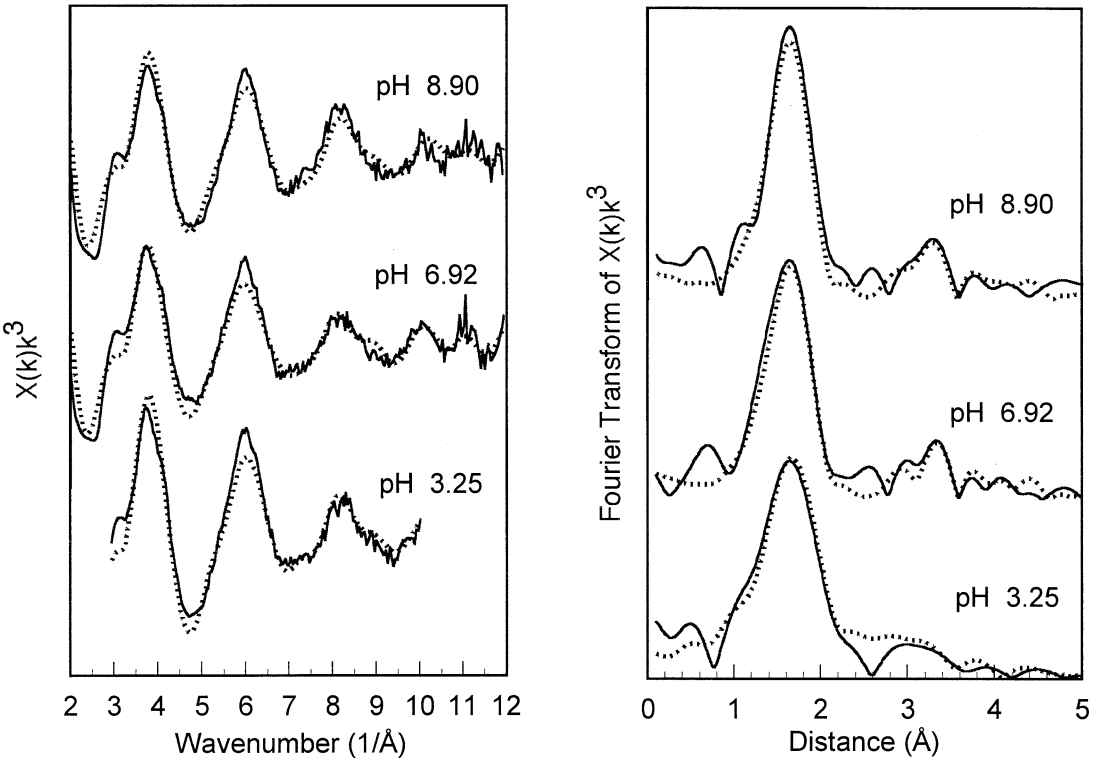

Fig. 6. EXAFS and Fourier transform of EXAFS for V(V) adsorption samples equilibrated with 25 ppm $[V]_{total}$.

The amphoteric treatment of a single surface site is generally recognised as a convenient modelling framework rather than a precise representation of actual functional groups existing at the mineral surface (Rustad et al., 1996). For iron oxyhydroxides in particular, a crystallographic consideration of the cleaved mineral surface (Hiemstra et al., 1989a, 1989b) shows surface oxide ions to be coordinated by up to three metal ions. As such, reactions 2 and 3 underestimate somewhat the complexity of a mineral surface. However, there has been considerable success in modelling cation (and anion) sorption under this construct, particularly when a single-site multispecies approach is applied (e.g., using the constant capacitance model: Palmqvist et al., 1997; using the DLM: Dzombak and Ali, 1996; using the TLM: Kosmulski, 1996). Recently, cation sorption data, previously modelled in a two-site or multisite approach, has been successfully remodelled in a single-site (multispecies) extended TLM framework (Criscenti and Sverjensky, 2002).

The DLM (Dzombak and Morel, 1990) and TLM (Hayes and Leckie, 1987; Hayes et al., 1988) were used to describe the electric double layer properties of the mineral surface. Mineral surface area and active surface site density were determined by BET analysis and a crystallographic consideration of the mineral surface respectively. Surface complexation involving ions of the background electrolyte was considered within the TLM framework, where NO_3^- and Na^+ were allowed to form outer sphere complexes at the β plane (Eqn. 4 and 5 in Table 2).

3.2.2. *Modelling potentiometric titration data*

The DLM has three adjustable model parameters; a surface site density and two acidity constants. We determined a unique

Table 1. Multiple scattering EXAFS fits for V(V) sorbed to goethite.

pH	R(V-O_1)$2\sigma^2$ Å^2)	R(V-O_2) ($2\sigma^2$ Å^2)	R(V-O_3) ($2\sigma^2$Å^2)	R(V-O_4) ($2\sigma^2$Å^2)	R(V-Fe_1) ($2\sigma^2$ Å^2)	R(V-Fe_2) ($2\sigma^2$ Å^2)	X^2 (R %)
			$[V]_{tot}$ = 2.5 ppm V(V)				
2.85	1.53 (0.012)	1.64 (0.001)	1.70 (0.001)	1.81 (0.001)	3.22 (0.006)	3.28 (0.002)	2.94 (27.0)
6.20	1.56 (0.025)	1.63 (0.001)	1.71 (0.001)	1.79 (0.001)	3.23 (0.005)	3.29 (0.003)	2.45 (25.0)
8.30	1.52 (0.001)	1.68 (0.001)	1.72 (0.001)	1.75 (0.001)	3.21 (0.005)	3.25 (0.003)	2.52 (24.6)
			$[V]_{tot}$ = 25 ppm V(V)				
3.25	1.54 (0.014)	1.63 (0.001)	1.71 (0.002)	1.80 (0.002)	3.22 (0.006)	3.29 (0.001)	3.91 (26.4)
6.92	1.57 (0.009)	1.65 (0.001)	1.74 (0.002)	1.79 (0.003)	3.24 (0.007)	3.28 (0.001)	2.58 (28.6)
8.90	1.59 (0.016)	1.62 (0.001)	1.73 (0.003)	1.77 (0.002)	3.23 (0.006)	3.28 (0.001)	2.64 (30.8)

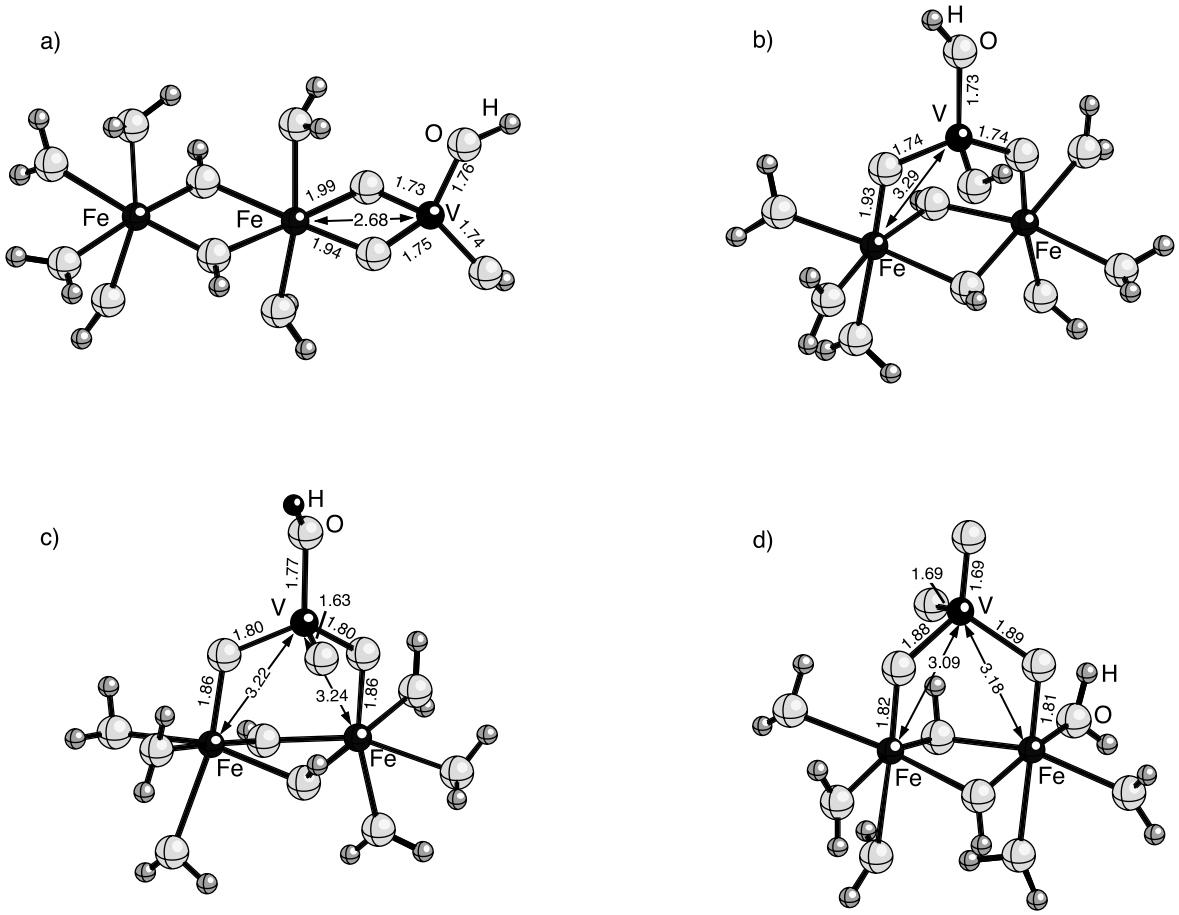

Fig. 7. V(V) ab initio molecular geometry clusters: (a) $VO_2(OH)_2$ bidentate edge-sharing (210), (b) $VO_2(OH)_2$ bidentate corner-sharing (110), (c) $VO_3(OH)$ on bidentate corner (110), (d) VO_4 on bidentate corner (110). Bond lengths shown in Å. Clusters (b) and (c) are favoured energetically and give V-Fe and V-O bond lengths in good agreement with those observed in the EXAFS.

set of parameter values by fixing site density at the value recommended by Hiemstra and van Riemsdijk (1996) and fitting the surface acidity constants (Eqn. 2 and 3 in Table 2). On the {110} and {010} faces of goethite (setting Pbnm), there are 3.03 and 7.19 sites/nm^2 of surface hydroxyls. For both the potentiometric titration models and the surface complexation of V, we used a site density of 6.02 sites/nm^2 as proposed by Hiemstra and van Riemsdijk (1996). This implies a significant contribution from the {010} faces in addition to the {110} faces which would be possible if the {110} faces consisted of {010} and {100} steps.

The TLM has six fitting parameters: site density, four equilibrium constants (two surface acidity constants and two electrolyte binding constants), and the capacitance of the inner helmholtz plane, C_1. The capacitance of the outer helmholtz plane (C_2) was assumed to be 0.2 F/m^2 following Hayes et al. (1991), Katz and Hayes (1995a, 1995b) and Gao and Mucci (2001). Attempts to simultaneously fit all parameters did not converge thus we adopted the modelling approach of Hayes et al. (1991). We determined a unique set of parameter values by fixing the site density (as before) and the surface acidity constants (Eqn. 2 and 3 in Table 2) and fitting for capacitance C_1 and electrolyte binding constants (Eqn. 4 and 5 in Table 2). Surface acidity constants were then varied according to ΔpK_a ($-[(\log K^-) + (\log K^+)]$) to find the value of the electrolyte binding constants at the largest ΔpK_a to cause no change in the goodness of fit parameter ($V(Y)$). Hayes et al. (1991) include a detailed description of the procedure.

Optimised acid-base parameter combinations are listed in Table 3 and the potentiometric titration data with model fits shown on Figure 8. The experimental pH_{PZC} (the pH where the surface charge is zero) is the same ($\pm$0.03 pH units) for all three ionic strengths measured (Fig. 8). We report a pH_{PZC} of 8.5. This value lies within the range of reported experimental values (~7.5–9.5). Model fits of the acid-base data (Fig. 8) show the TLM produces a very good replication of the data; the DLM fit is less satisfactory.

3.2.3. Modelling V(V) adsorption data

The observed vanadium adsorption data was replicated in the DLM and TLM using the optimised acid-base parameter combinations (Table 3). Equilibria for reactions occurring in solution (Eqn. 6–9 in Table 2) were taken from Baes and Mesmer (1976). Adsorption modelling of V(V) at 2.5 ppm $[V]_{total}$ and 25 ppm $[V]_{total}$ employed solution species 6 to 8 and 6 to 9 (Table 2)

Table 2. Mineral-V surface complexation model reactions.

α-FeOOH surface		
Species	Mass action relation	Equilibrium constant
(1) SOH	SOH	—
(2) SOH_2^+	$SOH + H^+ = SOH_2^+$	K_{a1}
(3) SO^-	$SOH = SO^- + H^+$	K_{a2}
(4) $SO^- - Na^+$	$SOH + Na^+ = SO^-Na^+ + H^+$	K_{cat}
(5) $SOH_2^+ - NO_3^-$	$SOH + NO_3^- + H^+ = SOH_2^+NO_3^-$	K_{an}
V(V)		
Solution speciation		
(6) VO_2^+	$VO_4^{3-} + 4H^+ = VO_2^+ + 2H_2O$	$K_{Hyd\ 1}$ $(10^{28.86})^a$
(7) $H_2VO_4^-$	$VO_4^{3-} + 2H^+ = H_2VO_4^-$	$K_{Hyd\ 2}$ $(10^{21.77})^a$
(8) HVO_4^{2-}	$VO_4^{3-} + H^+ = HVO_4^{2-}$	$K_{Hyd\ 3}$ $(10^{13.67})^a$
(9) $V_3O_9^{3-}$	$3VO_4^{3-} + 6H^+ = V_3O_9^{3-} + 3H_2O$	$K_{Hyd\ 4}$ $(10^{72.12})^a$
(10) H_2O	$H_2O = 2OH^- + H^+$	K_W $(10^{-13.79})^b$
Surface complexes		
(11) $SOVO_2H^+$	$SOH + VO_4^{3-} + 4H^+ = SOVO_2H^+ + 2H_2O$	K_{11}
(12) $SOVO_2^0$	$SOH + VO_4^{3-} + 3H^+ = SOVO_2^0 + 2H_2O$	K_{12}
(13) $SOH_2VO_3^0$	$SOH + VO_4^{3-} + 3H^+ = SOH_2VO_3^0 + H_2O$	K_{13}
(14) $SOHVO_3^-$	$SOH + VO_4^{3-} + 2H^+ = SOHVO_3^- + H_2O$	K_{14}
(15) $SOVO_3^{2-}$	$SOH + VO_4^{3-} + H^+ = SOVO_3^{2-} + H_2O$	K_{15}
(16) $S_2O_2V(OH)_2^+$	$2SOH + VO_4^3 + 4H^+ = S_2O_2V(OH)_2^+ + 2H_2O$	K_{16}
(17) $S_2O_2VO(OH)^0$	$2SOH + VO_4^{3-} + 3H^+ = S_2O_2VO(OH)^0 + 2H_2O$	K_{17}
(18) $S_2O_2VO_2^-$	$2SOH + VO_4^{3-} + 2H^+ = S_2O_2VO_2^- + 2H_2O$	K_{18}
Precipitates[c]		
(19) V_2O_5	$2VO_4^{3-} + 6H^+ = V_2O_5 + 3H_2O$	K_{19}
(20) $NaVO_3 \cdot 2H_2O$	$Na^+ + VO_4^{3-} + 2H^+ + H_2O = NaVO_3 \cdot 2H_2O$	K_{20}
(21) $Na_4V_2O_7 \cdot 18H_2O$	$4Na^+ + 2VO_4^{3-} + 2H^+ + 17H_2O = Na_4V_2O_7 \cdot 18H_2O$	K_{21}
(22) $Na_3VO_4 \cdot xH_2O$	$3Na^+ + VO_4^{3-} + xH_2O = Na_3VO_4 \cdot xH_2O$	K_{22}

[a] From Baes and Mesmer (1976).
[b] From Gunnarsson et al. (2000).
[c] From Kiehl and Manfredo (1937).

respectively. Adsorption of V(V) was modelled with VO_4^{3-}(aq) as the common basis component and the data was split into two adsorption regimes based on solution speciation (according to Baes and Mesmer, 1976). Adsorption from pH 1 to 4 was modelled with VO_2^+ as both the solution species (Eqn. 6 in Table 2) and the adsorbing species (Eqn. 11, 12 and 16 in Table 2). Adsorption from pH 4 to 12 was modelled with the successive hydrolysis products of VO_4^{3-} as both the solution species (Eqn. 7–9 in Table 2) and the adsorbing species (Eqn. 11–18 in Table 2).

Table 3. Acid-base fits used in mineral-V surface complexation modelling.

	DLM	TLM
pH_{PZC}[a]	8.5	8.5
Surface area (m^2/g)[b]	32.7	32.7
[SOH] (sites/nm^2)[c]	6.02	6.02
log K_{a1}[d]	6.78	7.5
log K_{a2}[d]	–10.10	–9.5
log K_{an}[d]		8.31
log K_{cat}[d]		–9.07
C_1 (F/m^2)[d]		1.0
C_2 (F/m^2)[e]		0.2
$V(Y)$[d]	85	9.8

[a] Determined from potentiometric titration data (this study).
[b] Determined from BET analysis (this study).
[c] Determined from a crystallographic consideration of the mineral surface (Hiemstra and van Riemsdijk, 1996).
[d] Determined from FITEQL simulation of potentiometric titration data (this study).
[e] From Katz and Hayes (1995a, 1995b).

3.2.4. V(V) complexation at the surface of goethite

A number of possible surface complexes (Eqn. 11–18 in Table 2) were modelled in the attempt to replicate the observed vanadium adsorption.

The DLM and TLM fit to the vanadium(V) adsorption data is shown on Figure 4 and summarised in Table 4. Although the acid-base data were replicated best by the TLM, both models are able to replicate the observed vanadium pH edge adsorption very well.

In both the DLM and TLM, surface species 11, 12 and 16 were considered singly and simultaneously for adsorption between pH 1 and 4 and species 11 to 18 were considered singly and in various combinations for adsorption between pH 4 to 12. In agreement with our EXAFS measurements and ab initio predicted geometries, we are able to fit the observed vanadium adsorption to the formation of $S_2O_2V(OH)_2^+$ (Eqn. 16 in Table 2) and $S_2O_2VO(OH)^0$ (Eqn. 17 in Table 2) surface complexes. Consistent with V(V) aqueous speciation (Fig. 3), we find $S_2O_2V(OH)_2^+$ surface complexes, formed from the adsorption and protonation of VO_2^+, provide an excellent fit to the experimental vanadium adsorption data at pH 1 to 4. At pH 4 to 12, we find $S_2O_2VO(OH)^0$ surface complexes, formed from the

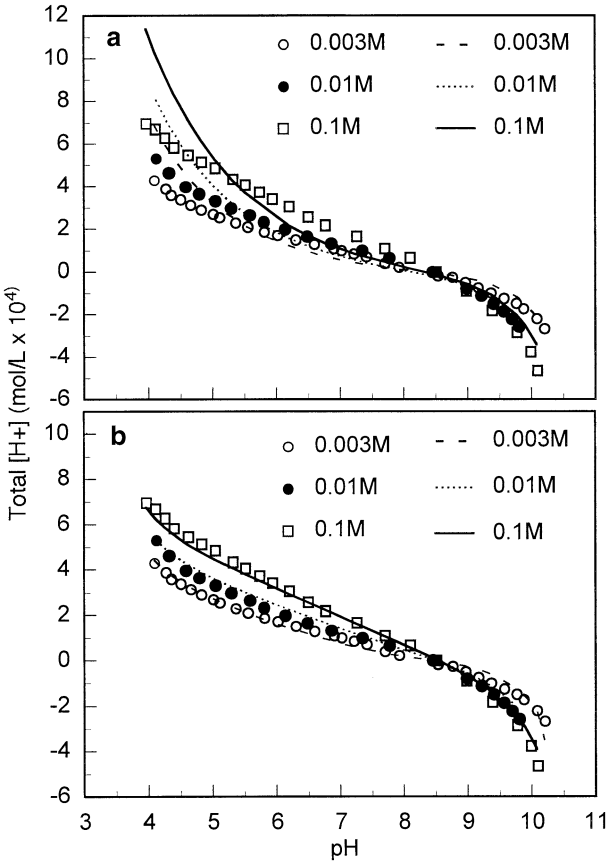

Fig. 8. Goethite potentiometric titration data at I = 0.003, 0.01 and 0.1 $NaNO_3$ and 25°C, shown as total $[H^+]$ in mol/L; 6.63 g/L oxide. Symbols are data points, lines are model fits: (a) DLM, (b) TLM.

adsorption of $VO_3(OH)^{2-}$ by ligand exchange, provide a similarly good match to the observed vanadium adsorption. In agreement with our EXAFS, it is unnecessary to employ a multispecies approach at each pH range to fit the experimental data.

The somewhat inhibited sorption between pH ~6 to 9 at 25 ppm $[V]_{total}$ is successfully modelled by including the formation of polynuclear $V_3O_9^{3-}$ in solution (Baes and Mesmer, 1976) which reduces the amount of $VO_2OH_2^-$ able to adsorb. We are also able to replicate the increased sorption above pH 9 at 25 ppm $[V]_{total}$ compared to 2.5 ppm $[V]_{total}$ (Fig. 4) by including the formation of sodium metavanadate (munirite, $NaVO_3 \cdot 2H_2O$) and sodium orthovanadate ($Na_3VO_4 \cdot xH_2O$) precipitates in solution which apparently form insoluble gels at high pH (Kiehl and Manfredo, 1937). A multispecies modelling approach was initially adopted but was unsuccessful. The increased sorption above pH 9 is of limited geochemical interest since at this pH regime we are outside the range of surface water and marine systems. The precipitates considered in modelling the observed vanadium adsorption at 25 ppm $[V]_{total}$ are listed in Table 2.

We also present modelling results (Table 5) for the description of our observed vanadium adsorption by monodentate surface complexes as put forward by Wehrli and Stumm (1989). At low pH (~1–4), Wehrli and Stumm (1989) proposed the formation of inner-sphere, monodentate $SOVO_2^0$ surface complexes via the adsorption of VO_2^+(aq) onto a single SOH surface site. These complexes are represented in our surface complexation modelling by Eqn. 12 in Table 2. At higher pH (~7–12), Wehrli and Stumm (1989) proposed the formation of inner-sphere, monodentate $SOVO_3H^-$ surface complexes via exchange of a single surface hydroxyl OH^- ligand for HVO_4^{2-}(aq). These complexes are represented in our modelling by Eqn. 14 in Table 2. Contrary to our direct spectroscopic evidence and ab initio predicted geometries, we are able to fit the observed vanadium adsorption with similar (and slightly improved overall) $V(Y)$ to the formation of monodentate $SOVO_2^0$ and $SOVO_3H^-$ surface complexes (see Table 5 in comparison to Table 4). The successful modelling of the observed vanadium adsorption with monodenate surface complexes demonstrates that modelling alone cannot distinguish between otherwise plausible adsorption complexes (first demonstrated by Westall and Hohl, 1980). Our results thus highlight the necessity of spectroscopic data to unambiguously fit sorption edges to a surface complexation model.

3.2.5. *Alternative mass action relations*

We have derived alternative mass action relations with corresponding log K values for $S_2O_2V(OH)_2^+$ and $S_2O_2VO(OH)^0$ surface complexation at 2.5 ppm $[V]_{total}$ using the vanadium(V) hydrolysis constants of Baes and Mesmer (1976) and the surface complexation reactions as fit in FITEQL (Eqn. 16 and 17 in Table 2, with log K_{16} and log K_{17}, Table 4).

Using reactions $K_{Hyd\ 1}$ (Baes and Mesmer, 1976), K_{a1} (this study) and K_{16} (this study), we derive log $K(S_2O_2V(OH)_2^+)$ in terms of the reaction

$$2SOH_2^+ + VO_2^+ = S_2O_2V(OH)_2^+ + 2H^+ \qquad (4)$$

If we define K in terms of the concentration of surface sites per liter of solution, i.e.,

Table 4. Predicted complexation of V(V) to goethite.

Predicted metal complexes	DLM		TLM	
V(V)	2.5 ppm $[V]_{total}$	25 ppm $[V]_{total}$	2.5 ppm $[V]_{total}$	25 ppm $[V]_{total}$
log K_{16}[a]	42.87	42.99	44.53	42.95
$V(Y)$	2.7	0.14	4.2	5.3
log K_{17}[a]	41.26	37.51	41.45	38.31
$V(Y)$	6.3	17.1	6.7	8.9

[a] From simulation of V(V) sorption data (this study).

Table 5. Monodentate complexation of V(V) to goethite.

Predicted metal complexes	DLM		TLM	
V(V)	2.5 ppm $[V]_{total}$	25 ppm $[V]_{total}$	2.5 ppm $[V]_{total}$	25 ppm $[V]_{total}$
log K_{12}[a]	32.31	32.51	31.05	30.39
$V(Y)$	4.3	2.4	1.2	0.2
log K_{14}[a]	28.66	26.40	29.20	25.92
$V(Y)$	1.2	12.8	5.9	3.3

[a] From simulation of V(V) sorption data (this study) with monodentate complexes as proposed by Wehrli and Stumm (1989).

$$K[S_2O_2V(OH)_2^+] = \frac{\{S_2O_2V(OH)_2^+\}[H]^2}{\{SOH_2^+\}^2[VO_2^+]} \quad (5)$$

then log $K(S_2O_2V(OH)_2^+)$ = 0.45 (in the DLM) or log $K(S_2O_2V(OH)_2^+)$ = 2.11 (in the TLM).

Similarly, using $K_{Hyd\ 3}$ (Baes and Mesmer, 1976), K_w (Gunnarsson et al., 2000) and K_{17} (this study) we derive log $K(S_2O_2VO(OH)^0)$ in terms of the reaction

$$2SOH + HVO_4^{2-} = S_2O_2VO(OH)^0 + 2OH^- \quad (6)$$

For $K(S_2O_2VO(OH)^0)$ defined in terms of the concentrations of surface sites/L, i.e.,

$$K[S_2O_2VO(OH)^0] = \frac{\{S_2O_2VO(OH)^0\}[OH^-]^2}{\{SOH\}^2[HVO_4^{2-}]} \quad (7)$$

we calculate log $K(S_2O_2VO(OH)^0)$ = 0.01 (DLM) or 0.2 (TLM).

We can also derive the first acid dissociation constant (K_{HA}) of the $S_2O_2V(OH)_2^+$ surface complex:

$$S_2O_2V(OH)_2^+ = S_2O_2VO(OH)^0 + H^+ \quad (8)$$

Using log $K(S_2O_2V(OH)_2^+)$ and log $K(S_2O_2VO(OH)^0)$, log K_{a1} (this study), log K_w (Gunnarsson et al., 2000), and V(V) hydrolysis constants (Baes and Mesmer, 1976) we calculate log K_{HA} = −1.61 (DLM) or −3.08 (TLM).

4. CONCLUSIONS

We measured the sorption of V(5+) onto goethite under oxic (P_{O2} = 0.2 bar) atmospheric conditions. The surface complexes for adsorption were determined using EXAFS spectroscopy and predicted from ab initio molecular geometries. The adsorption of V(V) onto goethite at pH ~6 to 9 has a concentration dependence that reflects the formation of polynuclear complexes in solution when $[V]_{total} > 2.5$ ppm. V(V) adsorbs on the α-FeOOH surface as the mononuclear VO_2^+ and $VO_3(OH)^{2-}$ ions (at low and high pH respectively). Adsorption occurs by the formation of inner-sphere surface complexes resulting from bidentate corner-sharing between doubly and singly protonated VO_4^{3-} tertrahedra and FeO_6 polyhedra. Having identified the $Fe_2O_2V(OH)_2^+$ and $Fe_2O_2VO(OH)^0$ surface complexes, we are able to fit the experimental vanadium(V) adsorption data to the reactions

$$2FeOH_2^+ + VO_2^+ = Fe_2O_2V(OH)_2^+ + 2H^+$$

and

$$2FeOH + HVO_4^{2-} = Fe_2O_2VO(OH)^0 + 2OH^-$$

Our modelling results highlight the necessity of spectroscopic data to unambiguously fit sorption edges to a surface complexation model.

Acknowledgments—Thanks are due to P. Chung Choi for assistance with ICP-AES analysis, Paul Moir-riche and Chris Corrigan at Daresbury Materials Support Laboratory for XRD, and Nick Chinnery at Daresbury Laboratory for support at station 8.1. Caroline Peacock also wishes to thank Leonard Simmons for helpful discussion and encouragement.

Associate editor: M. L. Machesky

REFERENCES

Auger Y., Bodineau L., and Leclercq S. (1999) Some aspects of vanadium and chromium chemistry in the English Channel. *Cont. Shelf Res.* **19,** 2003–2018.

Baes C. F. and Mesmer R. E. (1976) *The Hydrolysis of Cations*. John Wiley, New York.

Binsted N. (1998) *EXCURV98: The Manual*. CLRC Daresbury Laboratory, Warrington, UK.

Breit G. N. (1995) Origin of clay minerals associated with V-U deposits in the Entrada Sandstone, Placerville Mining District, Southwestern Colorado. *Econ. Geol.* **90,** 407–419.

Breit G. N, Goldhaber M. B (1989) Hematite-enriched sandstones and chromium-rich clays—clues to the origin of vanadium-uranium deposits in the Morrison Formation, southwestern Colorado and southeastern Utah. Vienna, Austria, International Atomic Energy Agency, Technical Document 500, 201–226.

Criscenti L. J. and Sverjensky D. A. (2002) A single-site model for divalent transition and heavy metal. Adsorption over a range of metal concentrations. *J. Colloid Interface Sci.* **253,** 329–352.

Cruywagen J. J. and Heyns J. B. B. (1991) Vanadium (V) equilibria. Spectrophotometric and enthalpimetric investigation of the dimerization and deprotonation of HVO_4^{2-}. *Polyhedron* **10 (*2*),** 249–253.

Dent A. J. and Mosselmans J. F. W. (1992) *A Guide to EXBACK, EXCALIB and EXCURV92*. CLRC Daresbury Laboratory, Warrington, UK.

Dzombak D. and Morel F. M. M. (1990) *Surface Complexation Modelling Hydrous Ferric Oxide*. John Wiley, New York.

Dzombak D. A. and Ali M. A. (1996) Effects of simple organic acids on sorption of Cu^{2+} and Ca^{2+} on goethite. *Geochim. Cosmochim. Acta* **60,** 291–304.

Elderfield H. and Schultz A. (1996) Mid-ocean ridge hydrothermal fluxes and the chemical composition of the ocean. *Ann. Rev. Earth Planet. Sci.* **24,** 191–224.

Gans P. and O'Sullivan B. (2000) GLEE: A new computer program for glass electrode evaluation. *Talanta* **51,** 33–37.

Gao Y. and Mucci A. (2001) Acid base reactions, phosphate and arsenate complexation, and their competitive adsorption at the surface of goethite in 0.7 M NaCl solution. *Geochim. Cosmochim. Acta* **65,** 2361–2378.

Gunnarsson M., Jakobsson A., Ekberg S., Albinsson Y., and Ahlberg E. (2000) Sorption studies of cobalt(II) on colloidal hematite using

potentiometry and radioactive tracer technique. *J. Colloid Interface Sci.* **231,** 326–336.

Hayes K. F. and Leckie J. O. (1987) Modelling ionic-strength effects on cation adsorption at hydrous oxide-solution interfaces. *J. Colloid Interface Sci.* **115,** 564–572.

Hayes K. F., Papelis C., and Leckie J. O. (1988) Modelling ionic-strength effects on anion adsorption at hydrous oxide-solution interfaces. *J. Colloid Interface Sci.* **125,** 717–726.

Hayes K. F., Redden G., Ela W., and Leckie J. O. (1991) Surface complexation models: An evaluation of model parameter estimation using FITEQL and oxide mineral titration data. *J. Colloid Interface Sci.* **142,** 448–469.

Hedin L. and Lundqvist S. (1969) Effects of electron-electron and electron-photon interaction on the one-electron states of solids. *Solid-State Phys.* **23,** 1–181.

Herbelin A. and Westall J. (1996) *A Computer Program for Determination of Chemical Equilibrium Constants From Experimental Data. Version 3.2*. Department of Chemistry, Oregon State University, Corvallis, OR.

Hiemstra T. and van Riemsdijk W. H. (1996) A surface structural approach to ion adsorption: The charge distribution (CD) model. *J. Colloid Interface Sci.* **179,** 488–508.

Hiemstra T., van Riemsdijk W. H., and Bolt H. (1989a) Multisite proton adsorption modeling at the solid/solution interface of (hydr) oxides: A new approach. Part I. *J. Colloid Interface Sci.* **133,** 91–104.

Hiemstra T., de Wit J. C. M., and van Riemsdijk W. H. (1989b) Multisite proton adsorption modeling at the solid/solution interface of (hydr) oxides: A new approach. Part II. *J. Colloid Interface Sci.* **133,** 105–117.

Hohl H. and Stumm W. (1976) Interaction of Pb^{2+} with hydrous γ-Al_2O_3. *J. Colloid Interface Sci.* **55,** 281–288.

Ikhsan J., Johnson B., and Wells J. D. (1999) A comparative study of the adsorption of transition metals on kaolinite. *J. Colloid Interface Sci.* **217,** 403–410.

Jung J., Cho Y., and Hahn P. (1998) Comparative study of Cu^{2+} adsorption on goethite, hematite and kaolinite: mechanistic modelling approach. *Bull. Korean Chem. Soc.* **19,** 324–327.

Katz L. E. and Hayes K. F. (1995a) Surface complexation modeling. I. Strategy for modeling monomer complex formation at moderate surface coverage. *J. Colloid Interface Sci.* **170,** 477–490.

Katz L. E. and Hayes K. F. (1995b) Surface complexation modeling. II. Strategy for modeling polymer and precipitation reactions at high surface coverage. *J. Colloid Interface Sci.* **170,** 491–501.

Keeney-Kennicutt W. L. and Morse J. W. (1984) The interaction of Np(V)O2+ with common mineral surfaces in dilute aqueous solutions and seawater. *Mar. Chem.* **15,** 133–150.

Kiehl S. J. and Manfredo E. J. (1937) A study of heterogeneous equilibria in aqueous solutions of the sodium salts of the vanadic acids at 30°. *J. Am. Chem. Soc.* **59,** 2118–2126.

Kosmulski M. (1996) Adsorption of cadmium on alumina and silica: Analysis of the values of stability constants of surface complexes calculated for different parameters of triple layer model. *Colloids Surf. A* **117,** 201–214.

Langmuir D. (1997) *Aqueous Environmental Geochemistry*. Prentice-Hall, London, UK.

Lovgren L., Sjoberg S., and Schindler P. W. (1990) Acid/base reactions and Al(III) complexation at the surface of goethite. *Geochim. Cosmochim. Acta* **54,** 1301–1306.

Lumsdon D. G. and Evans L. J. (1994) Surface complexation model parameters for goethite (α-FeOOH). *J. Colloid Interface Sci.* **164,** 119–125.

Northrop H. R. and Goldhaber M. B. (1990) Genesis of tabular-type vanadium-uranium deposits of the Henry basin, Utah. *Econ. Geol.* **85,** 215–269.

Palmqvist U., Ahlberg E., Lövgren L., and Sjöberg S. (1997) In situ voltammetric determinations of metal ions in goethite suspensions: Single metal ion systems. *J. Colloid Interface Sci.* **196,** 254–266.

Perdew J. P., Chevary J. A., Vosko S. H., Jackson K. A., Pederson M. R., Singh D. J., and Fiolhais C. (1992) Atoms, molecules, solids, and surfaces—applications of the generalised gradient approximation for exchange and correlation. *Phys. Rev. B* **46,** 6671–6687.

Robertson A. P. and Leckie J. O. (1998) Acid/base, copper binding, and Cu^{2+}/H^+ exchange properties of goethite, an experimental and modelling study. *Environ. Sci. Technol.* **32,** 2519–2530.

Rustad J. R., Felmy A. R., and Hay B. P. (1996) Molecular statics calculations of proton binding to goethite surfaces: A new approach to estimation of stability constants for multisite surface complexation models. *Geochim. Cosmochim. Acta* **60,** 1563–1576.

Schwertmann U. and Cornell R. M. (1991) *Iron Oxides in the Laboratory*. VCH Verlag, New York.

Schwertmann U. and Pfab G. (1996) Structural vanadium and chromium in lateritic iron oxides: Genetic implications. *Geochim. Cosmochim. Acta* **60,** 4279–4283.

Sherman D. M. (1985) Electronic structures of Fe3+ coordination sites in iron oxides: applications to spectra, bonding and magnetism. *Phys. Chem. Miner.* **12,** 161–175.

Sherman D. M, Randall S. R (2003) Surface complexation of arsenic(V) to iron(III) oxide hydroxides: Structural mechanism from density functional calculations and EXAFS spectroscopy. *Geochim. Cosmochim. Acta* **67,** 4223–4230.

Sigg L. and Stumm W. (1980) The interactions of anions and weak acids with the hydrous goethite (α-FeOOH) surface. *Colloids Surf.* **2,** 101–117.

Tadanier C. J. and Eick M. J. (2002) Formulating the charge-distribution multisite surface complexation model using FITEQL. *Soil. Sci. Soc. Am. J.* **66,** 1505–1517.

te Velde G., Bickelhaupt F. M., Baerends E. J., Fonseca Guerra C., van Gisbergen S. J. A., Snijders J. G., and Ziegler T. (2001) Chemistry with ADF. *J. Comput. Chem.* **22,** 931–967.

Trefry J. H. and Metz S. (1989) Role of hydrothermal precipitates in the geochemical cycling of vanadium. *Nature* **342 (***6249***),** 531–533.

Venema P., Hiemstra T., Weidler P. G., and van Riemsdijk W. H. (1998) Intrinsic proton affinity of reactive surface groups of metal (hydr)oxides: application to iron (hydr)oxides. *J. Colloid Interface Sci.* **198,** 282–295.

Vosko S. H., Wilk K., and Nusair M. (1980) Accurate spin-dependent electron liquid correlation energy for local spin density calculations: a critical analysis. *Can. J. Phys.* **58,** 1200–1205.

Wanty R. B. and Goldhaber M. B. (1992) Thermodynamics and kinetics of reactions involving vanadium in natural systems: Accumulation of vanadium in sedimentary rocks. *Geochim. Cosmochim. Acta* **56,** 1471–1483.

Wanty R. B., Goldhaber M. B., and Northrop H. R. (1990) Geochemistry of vanadium in an epigenetic sandstone-hosted vanadium-uranium deposit, Henry basin, Utah. *Econ. Geol.* **85,** 270–284.

Wehrli B. and Stumm W. (1988) Oxygenation of vanadyl(IV). Effect of coordinated surface hydroxyl groups and OH^-. *Langmuir* **4,** 753–758.

Wehrli B. and Stumm W. (1989) Vanadyl in natural waters: Adsorption and hydrolysis promote oxygenation. *Geochim. Cosmochim. Acta* **53,** 69–77.

Westall J. C. and Hohl H. (1980) A comparison of electrostatic models for the oxide/solution interface. *Adv. Colloid Interface Sci.* **12,** 265–294.